



**HAL**  
open science

# Beam-plasma interaction in randomly inhomogeneous plasmas and statistical properties of small-amplitude Langmuir waves in the solar wind and electron foreshock

K V Krasnoselskikh, V V Lobzin, K Musatenko, J S Soucek, J S Pickett, I H Cairns

► **To cite this version:**

K V Krasnoselskikh, V V Lobzin, K Musatenko, J S Soucek, J S Pickett, et al.. Beam-plasma interaction in randomly inhomogeneous plasmas and statistical properties of small-amplitude Langmuir waves in the solar wind and electron foreshock. *Journal of Geophysical Research Space Physics*, 2007, 112, pp.10109 - 10109. 10.1029/2006JA012212 . insu-01408841

**HAL Id: insu-01408841**

**<https://insu.hal.science/insu-01408841>**

Submitted on 5 Dec 2016

**HAL** is a multi-disciplinary open access archive for the deposit and dissemination of scientific research documents, whether they are published or not. The documents may come from teaching and research institutions in France or abroad, or from public or private research centers.

L'archive ouverte pluridisciplinaire **HAL**, est destinée au dépôt et à la diffusion de documents scientifiques de niveau recherche, publiés ou non, émanant des établissements d'enseignement et de recherche français ou étrangers, des laboratoires publics ou privés.



## Beam-plasma interaction in randomly inhomogeneous plasmas and statistical properties of small-amplitude Langmuir waves in the solar wind and electron foreshock

V. V. Krasnoselskikh,<sup>1</sup> V. V. Lobzin,<sup>1,2</sup> K. Musatenko,<sup>1</sup> J. Soucek,<sup>3</sup> J. S. Pickett,<sup>4</sup> and I. H. Cairns<sup>5</sup>

Received 7 December 2006; revised 23 July 2007; accepted 7 August 2007; published 26 October 2007.

[1] A numerical model for wave propagation in an unstable plasma with inhomogeneities is developed. This model describes the linear interaction of Langmuir wave packets with an electron beam and takes into account the angular diffusion of the wave vector due to wave scattering on small-amplitude density fluctuations, as well as suppression of the instability caused by the removal of the wave from the resonance with particles during crossing density perturbations of relatively large amplitude. Using this model, the evolution of the wave packets in inhomogeneous plasmas with an electron beam is studied. To analyze data obtained both in space experiments and numerical modeling, a Pearson technique was used to classify the spectral density distributions. It was shown that both experimental distributions obtained within the Earth's foreshock aboard the CLUSTER spacecraft and model distributions for the logarithm of wave intensity belong to Pearson type IV rather than normal. The main reason for deviations of empirical distributions from the normal one is that the effective number of regions where the waves grow is not very large and, as a consequence, the central limit theorem fails to be true under the typical conditions for the Earth's electron foreshock. For large amplitudes, it is suggested that power law tails can result from variations of wave amplitudes due to changes of group velocity in the inhomogeneous plasma, in particular due to reflection of waves from inhomogeneities.

**Citation:** Krasnoselskikh, V. V., V. V. Lobzin, K. Musatenko, J. Soucek, J. S. Pickett, and I. H. Cairns (2007), Beam-plasma interaction in randomly inhomogeneous plasmas and statistical properties of small-amplitude Langmuir waves in the solar wind and electron foreshock, *J. Geophys. Res.*, *112*, A10109, doi:10.1029/2006JA012212.

### 1. Introduction

[2] From the beginning of space research onboard satellites Langmuir waves have been the object of intensive studies in the solar wind, within the Earth's electron foreshock, and in the vicinity of other planetary shocks. These waves are generated as a result of the beam-plasma interaction. The early experimental studies of these processes were carried out in the source regions of the type III solar radio bursts. Detailed direct in situ measurements at 1 AU have shown the simultaneous occurrence of a bump on tail electron distributions and an increase of plasma wave level above the background [Lin *et al.*, 1981]. There were no indications of any of the plateau-type particle distribution predicted by quasilinear theory. From the very beginning it was pointed out that plasma waves are clumped into spikes

with peak amplitudes typically three orders of magnitude above the mean [Gurnett *et al.*, 1978]. The question arose whether these observations can be interpreted in terms of nonlinear wave packets, solitons, or wave collapse [Smith, 1977], because the major results of theoretical studies of weak and strong turbulence were already published at that time. Smith and Sime [1979] analyzed Langmuir waves in type III solar radio bursts sources in the solar wind. They pointed out that there is no evidence of any strong nonlinear phenomena such as soliton formation or collapse in the experimental data. They proposed the explanation of the clumping phenomenon based on the idea that the plasma is inhomogeneous, and in most regions where the beam could excite the waves the characteristic scale of the inhomogeneity is comparable with the spatial growth rate, thereby resulting in suppression of the instability. They argue that sufficient amplification occurs only along certain paths where by chance successive inhomogeneities are sufficiently similar that they do not interfere with the amplification process leading to the observed spikes. This idea was further developed by Muschietti *et al.* [1985], Melrose *et al.* [1986], Robinson [1992, 1995], and Robinson *et al.* [1993a, 1993b, 2004].

<sup>1</sup>LPCE/CNRS-Université d'Orléans, Orléans, France.

<sup>2</sup>le Studium Institute for Advanced Studies, Orleans, France.

<sup>3</sup>Institute of Atmospheric Physics, Prague, Czech Republic.

<sup>4</sup>University of Iowa, Iowa, USA.

<sup>5</sup>University of Sydney, Sydney, Australia.

[3] A very similar problem of beam-plasma interaction was studied in a laboratory plasma. The effect of density fluctuations was found to be important for the development of the instability and *Nishikawa and Ryutov* [1976] suggested that the major effect of small amplitude density fluctuations can be taken into account in the form of effective angular diffusion of the wave vector, which in turn results in the deviation of the wave phase velocity and quenching the instability. This approach was used in further studies in space and laboratory plasmas.

[4] The observations of the large scale electron density fluctuations in the solar wind gave strong argument in favor of such an interpretation. In situ measurements of the density fluctuations spectrum onboard ISEE 1 and 2 satellites [*Celnikier et al.*, 1983] revealed that characteristic density fluctuations as high as  $\delta n/n \sim 10^{-2}$  may exist on the scale range of the order of 100 km, while interplanetary scintillations measurements from extragalactic radio sources give an average value for  $\delta n/n$  of the order of  $10^{-3}$  [*Cronyn*, 1970]. In an ISEE propagation experiment, under typical conditions for solar wind at 20  $R_E$ , *Celnikier et al.* [1983] also found that the electron density power spectrum is not fit by a single power law in the entire frequency range from  $10^{-3}$  Hz to 5 Hz. Rather, there are two frequency ranges with different spectral indices, with the spectra showing the fracture at  $6 \cdot 10^{-2}$  Hz. Later on, for a considerably larger data set, *Celnikier et al.* [1987] confirmed their previous conclusion about two power laws with a transition point at about 0.1 Hz. They also argued that the power index for high frequencies is variable, while for low frequencies the index is approximately constant, and the absolute value of density fluctuations is proportional to the mean plasma density. The main contribution to the fluctuation level comes from high frequencies, for frequency range 4–16 Hz the mean relative fluctuation is as large as 0.04. In addition, *Celnikier et al.* [1987] found no evidence of a strong anisotropy of density fluctuations. Recently, *Kellogg and Horbury* [2005] have deduced density fluctuation spectra from EFW probe potential variations measured aboard Cluster spacecraft in the free solar wind. Because the observed electric fields accompanying these fluctuations are quite low, *Kellogg and Horbury* [2005] argue that electron and ion fluctuations are canceled out and resulting charge separations are small. Thus the fluctuations resemble ion acoustic waves [*Kellogg and Horbury*, 2005].

[5] The presence of such fluctuations can result in several physical effects that can affect beam-plasma interaction dynamics. Certain effects were identified recently making use of direct measurements of high frequency electric fields in space. *Bale et al.* [1998] and *Kellogg et al.* [1999] have reported that the waves observed in the vicinity of the electron foreshock region have quite often elliptical polarization, rather than linear, and can belong to the Z-mode rather than the Langmuir mode. They suggested that the transformation of primarily generated Langmuir waves to the slow electromagnetic mode can occur due to plasma inhomogeneities. *Bale et al.* [2000] have studied the dependence of wave amplitudes upon the ratio of the beam speed to the thermal electron velocity and have found that there is no direct correlation between the intensity of waves and characteristic energy of beams. *Bale et al.* [1997] pointed

out that presumably the probability distribution of wave intensity dependence should be separated on two parts. Small-amplitude waves can have the distribution related to linear instability properties while large-amplitude wave statistics described by a power law tail can be determined by nonlinear processes. An additional observational evidence of the role of nonlinear processes for large-amplitude wave statistics was presented by *Soucek et al.* [2005].

[6] Intensive studies of experimental probability distributions of wave energy were initiated by the development and application of stochastic growth theory (SGT) [*Robinson*, 1992, 1995; *Robinson et al.*, 1993a, 1993b; *Cairns and Robinson*, 1997, 1999]. The main idea of the SGT consists of the suggestion that the presence of large-amplitude density fluctuations results in the existence of finite regions where the instability occurs, similar to what was stated by previous authors. This gives rise to a statistical distribution of the growth rate, which in the limiting case, assuming a central limit theorem holds, results in lognormal distribution for the wave intensity. This result was obtained under the assumption that the wave amplitudes don't reach the level at which nonlinear processes become active. Making use of different experimental data obtained aboard spacecraft, *Robinson et al.* [1993a, 1993b], *Cairns and Robinson* [1997, 1999], *Cairns et al.* [2000], and *Sigsbee et al.* [2004] have demonstrated that the distributions observed at a point closely resemble a lognormal in the majority of the foreshock. However, close to the foreshock boundary [*Cairns et al.*, 2000] and averaged over the foreshock [*Bale et al.*, 1997; *Cairns and Robinson*, 1997; *Boshuizen et al.*, 2001] the distributions appeared power law at high fields with  $P(E) \propto E^{-2}$ . Spatial variations in wave parameters and the relatively small number of field samples and periods analyzed made it difficult to assess deviations from lognormals in these analyses.

[7] Recent simulations, which include Langmuir-beam evolution in an inhomogeneous plasma background, incorporate angular scattering, and take into account nonlinear wave processes, demonstrate the evolution of the beam-plasma system to a final state predicted by the stochastic growth theory [*Li et al.*, 2006a, 2006b].

[8] It is worth noting that very similar problem was studied for many years in radio engineering in connection with the shot noise probability distributions. *Gilbert and Pollak* [1960] developed an analytical approach to evaluate the probability distributions of shot noise that consists of pulses having a predefined shape and dependent upon parameters that determine the characteristics of pulses. They have obtained the integral equation that allows one to find such a distribution for different types of pulses. However, in most interesting cases the equation can be solved only numerically, thus the problem how to characterize such distributions was kept open.

[9] The question we will address in our paper is: can one distinguish and quantitatively characterize the role of different effects such as the angular diffusion due to small-amplitude density fluctuations, linear growth of waves in strongly inhomogeneous plasma, and amplitude variations associated with the change of the wavelength due to variations of plasma density. For this purpose we suggest to use the Pearson technique of classification of different

distributions [Pearson, 1895]. A comparative analysis of distributions obtained from modeling and experimental measurements can allow identifying the relative role of different factors. Our work is the first step on quantifying physical processes with the use of such statistical approach, but the results obtained seem to be very promising.

[10] Presented in this paper experimental observations made aboard the CLUSTER spacecraft in the solar wind show that the probability density function for energy of small-amplitude Langmuir waves can deviate considerably from a lognormal distribution. In addition, a theoretical interpretation of these deviations and comparison of numerical simulation results with experimental data are provided.

[11] The remainder of the paper is organized as follows. Section 2 describes a numerical model for Langmuir wave growth/damping in the presence of an electron beam, a multitude of small-amplitude density fluctuations, and a single large-amplitude density inhomogeneity. This model is used to study the spatial evolution of a single plasma wave packet. In Section 3, the numerical model presented in the previous section is used to determine statistical parameters characterizing a spatial evolution of Langmuir waves in plasmas with a number of random large-amplitude inhomogeneities. Besides, this section describes a classification procedure of measured/modeled distributions by attributing them to one of a family of Pearson distributions. The results obtained both in numerical simulations and aboard the Cluster spacecraft in a vicinity of the Earth's foreshock boundary are briefly discussed in Section 4. The main conclusions of the paper are summarized in Section 5.

## 2. Numerical Model for Beam-Plasma Interaction in Randomly Inhomogeneous Plasmas

[12] To study the influence of random density inhomogeneities on the evolution of Langmuir waves resulting from the plasma-beam instability in space plasmas, we assume for simplicity that the inhomogeneities fall into two distinct types, namely relatively large-amplitude density disturbances and small-amplitude ones. Suppose further that these inhomogeneities have negligible velocities as compared to the group velocity of Langmuir waves and large characteristic spatial scales, the scale of large-amplitude fluctuations being larger than that of small-amplitude ones.

[13] To come to a more precise mathematical description, let us introduce the following notation. Let  $q$  and  $Q$  be typical "wave numbers" characterizing spatial scales of small-amplitude inhomogeneities and large-amplitude ones, respectively,  $\Delta n$  and  $\Delta N$  be the corresponding typical plasma density perturbations,  $k$  a typical wave number of unstable Langmuir waves,  $v_g$  and  $\Gamma$  the group velocity and growth rate for their energy, respectively.

[14] Let the characteristic spatial scales of both types of inhomogeneities be large as compared with the wavelength of plasma oscillations and the growth rate be sufficiently small,

$$Q < \Gamma/v_g \ll q \ll k.$$

In this case, we can introduce an average spectral density of Langmuir waves,  $\mathcal{W}$ , where the averaging is performed over

the space and time intervals  $\Delta r$  and  $\Delta t$  satisfying the conditions

$$1/qv_g \ll \Delta t \ll 1/\Gamma, 1/Qv_g$$

and

$$1/q \ll \Delta r \ll v_g/\Gamma, 1/Q. \quad (1)$$

From (1) it follows that the wave packets under consideration are more narrow than large-amplitude density inhomogeneities but extend over a lot of small-amplitude fluctuations.

[15] If for small-amplitude density fluctuations the condition

$$\Delta n/n \ll 3Tk^2/m\omega_{pe}^2$$

is satisfied, the Langmuir wave packets cannot be trapped by these inhomogeneities but only scattered. Moreover, the scattering is elastic (without changes of frequency and absolute value of wave vector) and diffusive if the inhomogeneities are randomly distributed in space and their velocities are negligible [Nishikawa and Ryutov, 1976]. For large-amplitude inhomogeneities, we assume that

$$\Delta N/n \lesssim 3Tk^2/m\omega_{pe}^2,$$

in other words, the magnitude of the wave vector can be changed significantly during crossing such an inhomogeneity but the inhomogeneity is not large enough to reflect the packet backwards.

[16] In summary, for small-amplitude density fluctuations the assumptions by Nishikawa and Ryutov [1976] are used, allowing us to treat these fluctuations as a stochastic process and calculate their influence in the Fokker-Plank approximation, while the interaction of a wave packet with each large-amplitude density disturbance should be considered in the framework of a deterministic approach. Thus the evolution of the waves is described by the equation

$$\frac{\partial W}{\partial t} + (\mathbf{v}_g \cdot \nabla) W = \Delta DW + \Gamma W,$$

where  $W$  is the wave spectral energy density.

[17] It is worth noting here several properties of the wave propagation in the presence of the growth/damping effects when the diffusion effect is negligible and some inhomogeneities are large enough to reflect the packets backwards,  $\Delta N/n \gtrsim 3Tk^2/m\omega_{pe}^2$ . The plasma density profile is assumed to be presented as a hypersurface having valleys and hills and the wave propagation corresponds to the motion of some "object" that flies at a certain constant height. When the object meets the hypersurface of the "land," it is reflected. Because of instability, the wave grows in amplitude while moving within some "cone," otherwise it damps. In addition, the wave amplitude can also change due to variations of group velocity. Such a picture corresponds to a WKB solution that can be written as

$$W(t, \mathbf{r}) = \frac{W_0}{\sqrt{|k_n|}} \exp\left(-i\omega t + i \int \mathbf{k} d\mathbf{r}\right),$$

where  $\mathbf{k}$  is a complex wave vector describing variations of both the wave phase and amplitude and  $k_n$  is the component of the wave vector perpendicular to the surface. In such a case the statistics of wave amplitudes is determined by the statistical properties of the plasma density profile and the initial value of the wave vector. There exist several different groups of waves, which can be classified as follows. The waves from the first group are trapped inside some valleys and cannot escape. They are localized in the vicinity of the three-dimensional density holes and their dynamics consists of periodical variations between damping and growth. The second group includes the waves that move in multiply-connected area and are reflected to rather arbitrary angles while touching the surface. The wave amplitude temporarily grows during reflection and on average the wave will mainly grow and damp in the presence of the growth/damping rate. An important change in the wave behavior happens if the effect of the diffusion on the small-amplitude density fluctuations becomes strong enough. In the case with negligible diffusion, the trajectories in general can intersect, however, the local amplitude behavior is determined by the waves that arrive from the ‘‘cone’’ of growth rate. In another case when the diffusion effect is large enough, the waves can arrive from any direction and the effects of the interference can also become important.

[18] The plasma inhomogeneities encountered by the wave packet influence the wave amplitude due to variations of the effective growth rate, refractive scattering, and variations of the group velocity. Indeed, consider a one-dimensional case in the approximation of geometrical optics and zero growth rate. Let  $x = 0$  be the point of reflection. The wave number  $k$  vanishes at  $x = 0$ . Assume that in a sufficiently large vicinity of this point  $k \propto x^{1/2}$ . We have  $v_g W = \text{const}$ , where  $W$  is the wave energy density. From the dispersion relation for Langmuir waves it follows that  $v_g \propto k$ , thus the wave energy is proportional to  $k^{-1}$ . By definition, the probability to observe the wave energy within the range from  $W$  to  $W + dW$  is  $P_W(W) dW$ . In the case of standing waves, there is a one-to-one correspondence between  $x$  and  $W$ , hence,  $P_W(W) dW = P_x(x) dx$ , where  $P_x(x) dx$  is the probability to make the measurements within given space interval. If we assume that the instrument moves with a constant velocity in the region of interest,  $P_x$  will be constant and after simple and straightforward calculations we get a power law distribution of wave energies,  $P_W(W) \propto W^{-3}$ . In the other case when the wave activity is composed of separate packets and these packets are oscillating between the points of reflection, the probability to observe the waves within given space region will be inversely proportional to its group velocity,  $P_x \propto v_g^{-1}$ , and we get  $P_W(W) \propto W^{-2}$ . Previous analyses yield  $P_W(W) \propto W^{-3}$  at high  $W$  for waves subject to refractive scattering by zero-mean, Gaussian density fluctuations along a raypath [Salpeter, 1967] and propagation of rays subject to a caustic [Cairns, 2004; M. A. Walker, personal communication, 2003]. Obviously, these mechanisms can change considerably the high-energy part of the distribution by forming a power law tail. However, a detailed study of this effect is beyond the scope of the present paper, where we will focus on the effects of diffusion and fluctuations of the growth rate and consider experimental data with small wave amplitudes and without power law tails.

[19] There exist two simplified approaches to study statistical properties of waves in unstable plasmas with inhomogeneities, i.e., with the use of a stationary boundary problem for wave propagation and a temporal one. In the first approach, a stationary state for wave energy density is considered, both the growth rate and wave spectra depending on coordinates. The second approach was used by Nishikawa and Ryutov [1976], who studied a temporal evolution of the waves in macroscopically homogeneous plasmas, without dependence on spatial coordinates. These two approaches have obvious similarity, however, in the present paper we choose the first one, which seems to be more convenient from a numerical point of view.

[20] Thus to simplify the problem, let us consider a stationary case, when Langmuir waves enter a half-space  $x > 0$  occupied by unstable nonuniform plasma and both the plasma parameters and solution depends only on one coordinate,  $x$ , and does not depend on time. Then the spatial evolution of the wave packet is governed by the equation

$$v_g \cos \theta \frac{\partial W}{\partial x} = \frac{1}{\sin \theta} \frac{\partial}{\partial \theta} \left( D \sin \theta \frac{\partial W}{\partial \theta} \right) + \Gamma W, \quad (2)$$

where  $\Gamma(x, k, \theta)$  is an effective damping/growth rate for wave energy and  $\theta$  is the angle between the axis  $x$  and wave vector. The influence of microscopic small-amplitude density fluctuations is described by the first term on the right-hand-side in (2), where  $D(x, k, \theta)$  is the diffusion coefficient.

[21] First of all, it is instructive to analyze effects of small-amplitude density fluctuations. In this case, wave packets with different wave numbers evolve independently. If we take a narrow range of wave numbers and assume that the fluctuation spectrum is isotropic, then the diffusion coefficient  $D$  is approximately constant and the growth rate depends only on  $x$  and  $\theta$ .

[22] Let  $\Gamma$  be a typical value of the growth rate in the region considered. From (2) we observe that two dimensionless parameters can be introduced,  $\delta_1 = \Gamma/D$  and  $\delta_2 = \Gamma \Delta x / v_g$ , where  $\Delta x$  is a characteristic length. The second parameter,  $\delta_2$ , characterizes the spatial growth/damping rate of the waves if the diffusion effects are negligible. More precisely, if we choose the angle  $\theta = 0$  and consider two points separated by a sufficiently small distance  $\Delta x$  such that  $\Gamma(x, 0)$  does not change considerably between the points chosen, the wave energies at these points will differ by a factor of  $\exp(\delta_2)$ , i.e.,

$$\delta_2 = \Delta x \left. \frac{\Delta \ln W}{\Delta x} \right|_{D=0}.$$

To evaluate the relative contribution of the growth/damping with respect to diffusion in the numerical simulations, it is natural to consider a ratio

$$R = \Delta x \frac{\Delta \ln W}{\Delta x} / \delta_2, \quad (3)$$

which can be introduced both for the spectral energy density  $W(x, \theta)$  and for the total wave energy density,

$$W_{\text{tot}} = 2\pi \int_0^\pi W(x, \theta) \sin \theta d\theta, \quad (4)$$

if the dependencies of  $W(x, \theta)$  and  $W_{\text{tot}}(x)$  on the distance are approximately exponential in the region considered. In particular, this is the case when the growth rate depends only on  $\theta$ , for example,

$$\frac{\Gamma(x, \theta)}{\Gamma_{\text{max}}} = -0.1 + 1.1 \exp \left[ -\frac{1}{2} \left( \frac{\theta}{\Delta\theta} \right)^2 \right]. \quad (5)$$

For numerical modeling, a finite difference approximation scheme was developed to solve the differential equation (2). Both the approximations and algorithm for solving the equations obtained are similar to those described by *Mishin et al.* [1990] and *Khazanov et al.* [1994].

[23] The results of calculations with the growth rate profile (5), where  $\Delta\theta = \pi/10$ , are shown in Figure 1, both for the spectral energy density  $W(x, \theta)$  and for the total wave energy density  $W_{\text{tot}}$ .

[24] It is easily seen from Figure 1a that for small ratios  $\Gamma_{\text{max}}/D$ , when diffusion dominates, the effective growth rate does not depend on the angle  $\theta$ , and the spectra should be isotropic. Moreover, in this case the instability ceases, in accordance with the results by *Nishikawa and Ryutov* [1976]. As  $\Gamma_{\text{max}}/D$  increases, an anisotropy of wave spectra becomes apparent, and when a threshold value of this ratio is exceeded, regions in  $\mathbf{k}$ -space appear with positive effective growth rate, and the instability develops. However, even if the ratio  $\Gamma_{\text{max}}/D$  is as large as 20, the effective growth rate of the instability is considerably smaller than that without diffusion. The second characteristic of the spectra are their angular width. As already mentioned above, the spectra are quasi-isotropic for small ratios of  $\Gamma_{\text{max}}/D$  and become narrower for larger values of this ratio. This statement is illustrated by Figure 1b, which shows the dependence of the angular half-width of the spectra,  $\Delta\theta_{\text{fin}}$ . The half-width is evaluated at the end of the simulation box,  $x = x_{\text{max}}$ , and is determined by  $W(x_{\text{max}}, \theta_{\text{fin}}) = W(x_{\text{max}}, 0)/2$ .

[25] When large-amplitude density fluctuations exist in the plasma, the wave vector of the Langmuir wave packet changes both in the direction and absolute value. Strictly speaking, Equation (2) does not hold in this case and should be replaced by a more general one. However, some qualitative aspects of the problem under consideration can be studied with the use of (2), where spatial variations of the growth rate are incorporated to take into account the effects of moving the wave out from resonance with an electron beam when the wave crosses a large-amplitude density inhomogeneity.

[26] Let

$$\frac{\Gamma(x, \theta)}{\Gamma_{\text{max}}} = -0.1 + 1.1 \exp \left[ -\frac{1}{2} \left( \frac{\theta}{\Delta\theta} \right)^2 \right] \exp \left[ -\frac{1}{2} \left( \frac{x - x_0}{\Delta x} \right)^2 \right], \quad (6)$$

where  $\Delta x$  is a characteristic spatial scale of the inhomogeneity. The growth rate given by (6) takes positive values in a vicinity of  $x_0$  and forward direction of propagation, while for large deviation from this direction and larger distances from  $x_0$  it approaches the same negative value. The results of numerical simulations with this profile are shown in Figure 2.

[27] It is easily seen that the width of the wave packet is more narrow than that of the growth rate and that the relative position of the maximum wave energy with respect to the peak of the growth rate depends on the ratio  $\Gamma_{\text{max}}/D$  – compare panels (a) and (b) in Figure 2. In particular, the shapes of wave packets are similar for different values of  $\Gamma_{\text{max}}/D$ , but there exist some substantial distinctions (see panel (c) in Figure 2, where shown are the packets after a shift such that the maxima of the packets become coincident). In particular, for relatively small  $\Gamma_{\text{max}}/D$  the packets are considerably asymmetrical. With the increase in  $\Gamma_{\text{max}}/D$ , the asymmetry vanishes, and, in addition, large parts of ascending and descending halves of the pulse become approximately exponential.

### 3. Numerical Modeling of Wave Propagation in Unstable Plasma With Inhomogeneities

[28] To study statistical properties of small-amplitude waves in randomly inhomogeneous plasmas, when nonlinear effects can be neglected, consider the following boundary value problem for Equation (2),

$$W|_{x=0} = W_0(\theta) \quad \text{for } 0 \leq \theta \leq \pi/2,$$

$$W|_{x=x_{\text{max}}} = 0 \quad \text{for } \pi/2 < \theta \leq \pi.$$

[29] It is assumed that for large  $x$  the instability ceases and Langmuir waves damp. The growth rate  $\Gamma(x, \theta)$  is a shot-noise-like function of  $x$ . More precisely,  $\Gamma(x, \theta)$  is a superposition of impulses with random positions. The mean number of impulses is chosen to be equal to 50 for all runs, but the exact number is random and follows the Poisson distribution. The impulses have the same shape given by (6) but different amplitudes, which are uniformly distributed between zero and the maximum value corresponding to  $\Gamma_{\text{max}}/D = 15$ . The ratio of the total width of the region occupied by large-amplitude inhomogeneities to the impulse width,  $\Delta x$ , is equal to the mean number of impulses, 50. Thus in the case considered the inhomogeneities overlap. However, for a given point there are only a few overlapping impulses.

[30] To estimate the probability density function of wave energy for given  $x > 0$ , we take the results of 10000 runs with different profiles of the growth rate, where both the number of impulses, their amplitudes and positions were chosen randomly, in accordance with the corresponding probability distributions.

[31] To describe the shape and other properties of the distributions obtained in the simulations, it is convenient to use a technique related to Pearson curves [*Pearson*, 1895]. This technique has three important advantages, i.e., it is objective, can be easily automated, and provide final results in a compact form [*Hahn and Shapiro*, 1967]. The corresponding procedure includes the following stages.

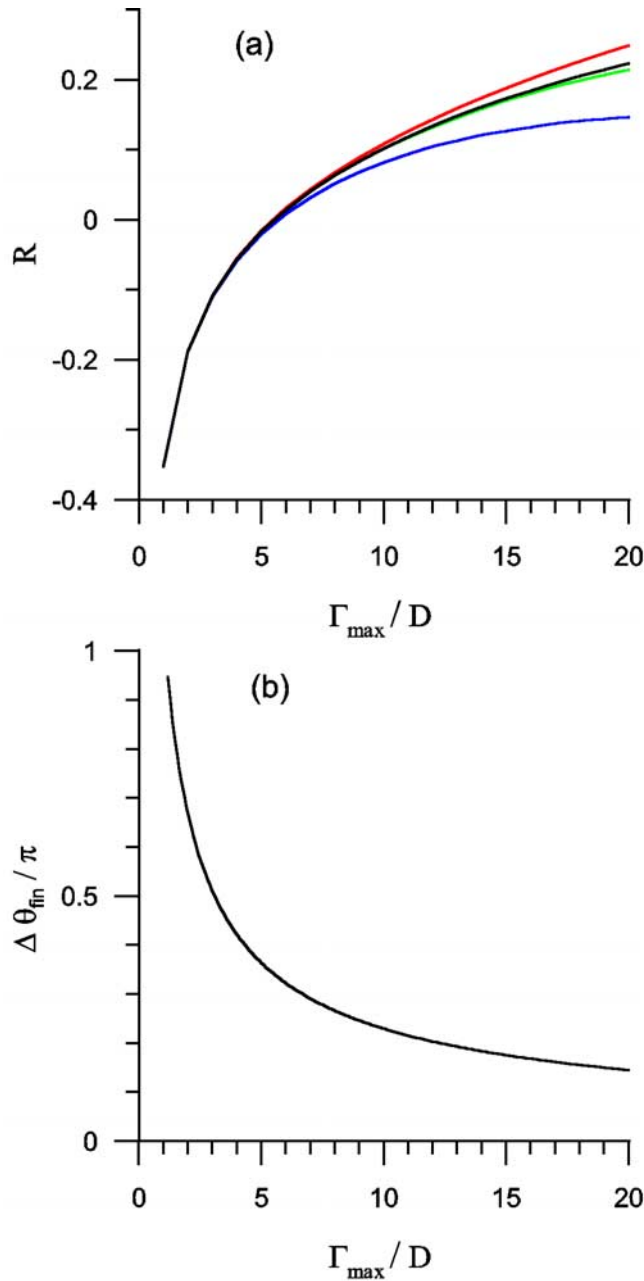


**Figure 1.** (a) The dependencies of normalized effective growth rates  $R$  (see (3) for definition) on the ratio  $\Gamma_{\max}/D$  for the Gaussian profile of the growth rate  $\Gamma(\theta)$  given by (5) with  $\Delta\theta = \pi/10$ . The black line shows the results for the total spectral energy  $W_{\text{tot}}$  (see (4) for definition). Red, green and blue lines represent the data derived for the spectral energy densities  $W(\theta, x)$ , where  $\theta = 0, \pi/2$ , and  $\pi$ , respectively. (b) The dependence of the final angle half-width of the wave spectra on the ratio  $\Gamma_{\max}/D$ .

From available data set, the first four moments are calculated. Assuming that these estimates are exact, an approximation of empirical distribution can be found by integrating a linear ordinary differential equation. The obtained fit can then be compared with the actual data to validate the results of fitting.

[32] The system of Pearson's curves describes wide classes of distributions having one single extremum. All of them are described by the differential equation

$$\frac{dp(z)}{dz} = \frac{z-a}{b_0 + b_1z + b_2z^2} p(z),$$

where  $a$  and  $b_i$  are constants [Hahn and Shapiro, 1967; Tikhonov, 1982; Podladchikova et al., 2003]. Thus these distributions are fully described by 4 parameters, which can be related to the mean and 3 moments about the mean,  $\mu_2$ ,  $\mu_3$ , and  $\mu_4$ . The shape of the distributions depend on 2 dimensionless parameters defined by

$$\beta_1 = \frac{\mu_3^2}{\mu_2^3}, \quad \beta_2 = \frac{\mu_4}{\mu_2^2}. \quad (7)$$

These parameters characterize the asymmetry (skewness) and the peakedness (kurtosis) of the distribution, respectively.

[33] Pearson [1895] suggested a classification of distributions with 12 classes, depending on parameters  $\beta_1$  and  $\beta_2$ . The top panel in Figure 3 contains the  $\beta_1 - \beta_2$  plane and shows the regions for some classes, namely, for beta distributions (region I), gamma distribution (line III), log-normal distribution (line V), and others (region IV). The normal distributions are represented by a single point  $\beta_1 = 0, \beta_2 = 3$ . For more details see, for example, Hahn and Shapiro [1967], Tikhonov [1982], Podladchikova et al. [2003] and references therein.

[34] The results deduced from numerical simulations are shown on the diagram in Figure 3 (top and middle panels) by a series of red circles. Each model data point is obtained from 10000 values of logarithm of wave energy density,  $\log_{10}W$ , at a fixed  $x$ . Different data points correspond to different distances from the boundary  $x = 0$ , and as a consequence, to a different mean number of growth rate impulses,  $N_{\text{imp}}$ , that the wave comes through. The error bars in the middle panel of Figure 3 show the statistical scatter for betas in the case of the null hypothesis that the logarithm of wave energy density obeys a normal distribution.

[35] From Figure 3 we observe that as  $N_{\text{imp}}$  increases, the data points approach the point representing normal distributions (black cross in the top and middle panels), in accordance with simple reasoning based on the central limit theorem. However, in general the deviations from a normal distribution are substantial, especially with respect to  $\beta_1$ .

[36] These findings can be interpreted in the framework of simple considerations outlined below.

[37] If then the wave diffusion is absent and the conditions for WKB approximation are satisfied, the wave energy density is given by

$$W(x) = W_0 \exp\left(\int_0^x \Gamma(x') dx'\right).$$

In plasmas with small-amplitude fluctuations, which scatter the waves, the growth rate for wave energy should be

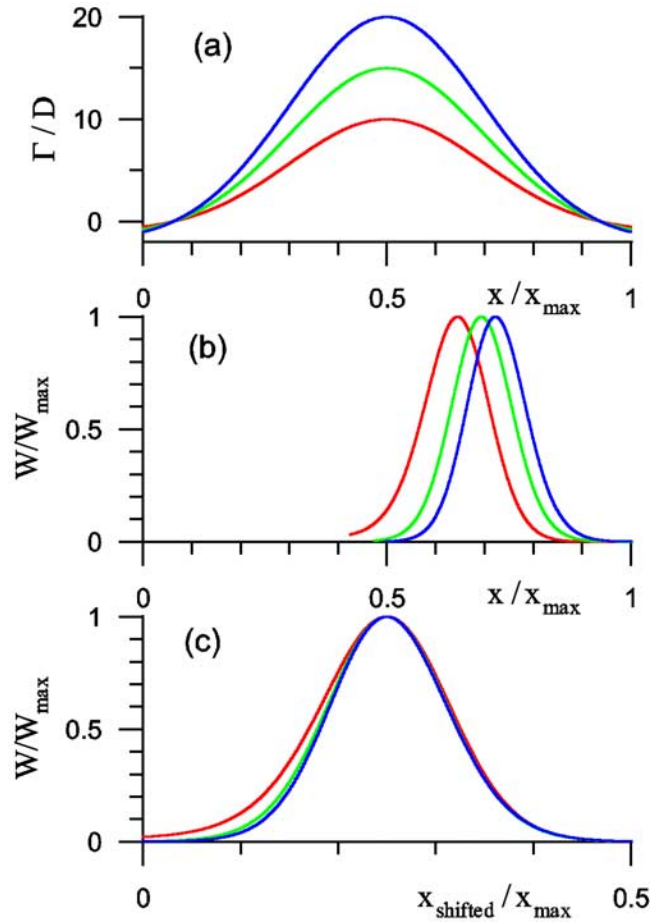


**Figure 2.** The results of numerical simulations of instability with a single large-scale inhomogeneity. (a) Spatial profiles of the ratio  $\Gamma/D$  for  $\theta = 0$  and different values of  $\Gamma_{\max}/D$ . (b) Spatial dependencies of normalized wave energy densities obtained for  $\Gamma_{\max}/D = 10$  (red line), 15 (green line) and 20 (blue line). (c) The profiles shown in panel (b) after spatial shifts such that the maximums of the curves coincide.

replaced by its effective value. If we suppose that the effective growth rate resembles a shot noise,

$$\Gamma(x) = \sum_{i=0}^{N_{\text{imp}}} F_{\Gamma}(a_i, x - x_i), \quad (8)$$

where the shape of each impulse is described by the same function depending on a parameter  $a_i$ , the positions of the impulses  $x_i$  form a Poisson sequence, and  $a_i$  are random and independent, then,  $\ln(W/W_0)$  is also a shot noise process of the same form,

$$\ln(W/W_0) = \sum_{i=0}^{N_{\text{imp}}} F_W(a_i, x - x_i), \quad (9)$$

where  $F_W(a, x) = \int_{-\infty}^x F_{\Gamma}(a, x') dx'$ .

[38] Finding the amplitude distribution of the shot noise of the form (8), as well as for a more simple case of noise composed of impulses with the same amplitude,

$$\Gamma(x) = \sum_{i=0}^{N_{\text{imp}}} F_{\Gamma}(x - x_i), \quad (10)$$

is very important both for theory and applications. *Rice* [1944] addressed this problem with  $F(a, t) = aF(t)$ , as well as for shot noise (8), and obtained an expression for the probability density function in the form of a Fourier integral. *Gilbert and Pollak* [1960] argued that the Rice solution can be easily evaluated only for nearly Gaussian noise, when the impulse rate is large. In their turn, they proved a theorem that finding the distribution for a noise given by (8) can be reduced to the same problem for (10). Then, for a shot noise given by (10) they obtained an integral equation for amplitude distribution and presented several examples when this equation can be solved analytically [Gilbert and Pollak, 1960]. However, in a general case this equation can be solved only with the use of numerical methods. *Gilbert and Pollak* [1960] presented one example of such calculations when the pulse shape is an exponentially damped high-frequency sinusoid,  $\exp(-t)\sin(\omega t)$ ,  $t \geq 0$ . They found noticeable differences in the tails of the normal distribution and calculated one, even for relatively high impulse rate of 10 impulses per unit time. For smaller impulse rates, the differences exist in the entire range of amplitudes.

[39] In summary, the theory developed by *Gilbert and Pollak* [1960] describes the way how the probability density function of the shot noise can be calculated when the shapes of the impulses are known together with statistical properties such as the impulse rate, amplitude distribution etc. In a general case, the application of this theory for interpretation of experimental data requires a lot of numerical calculations. On the other hand, when dealing with experiments, an inverse problem of deriving the properties of impulses from the noise observed may be even more interesting. That is why it is desirable to find other approaches that are easy to use and provide information that is not so detailed. One of such approaches, as was already mentioned above, is related to the first four moments of the distribution and Pearson curves.

[40] For simplicity assume that the domain occupied by random inhomogeneities is surrounded by the regions with  $\Gamma = 0$ , the shape for the effective growth rate within each inhomogeneity can be described by a finitely supported function, which vanishes outside a bounded interval, and there are no inhomogeneities in a vicinity of the point, where the measurements were performed. Then, from (9) it follows that  $\ln(W/W_0)$  can be represented as a sum of independent terms with the same statistical properties, in particular, with the same mean and variance. It follows from the central limit theorem that the distribution of this sum approaches the normal one as the number of terms increases. In the exceptional case of normally distributed terms the sum of any number of terms always follows the normal distribution. However, in general, the form of the distribution of the sum depends considerably on the details of term distributions provided the number of terms is not so

large. The skewness and curtosis of the sum is determined by the corresponding statistical properties of the terms. Without loss of generality, we can suppose that the mean values of each term are equal to zero. If this is not the case, the problem of convergence appears only for infinite regions, while for finite regions simple redefinitions of the variables are sufficient to reduce the problem to what follows.

[41] Let

$$W = \sum_{i=1}^n w_i,$$

where  $W$  is the normalized wave intensity and  $w_i$  is the contribution of the  $i$ th impulse. Obviously,

$$M_2 = n\mu_2 \text{ and } M_3 = n\mu_3,$$

where  $M_{2,3}$  are the second and third central moments for  $W$ . From simple combinatorial considerations it follows that

$$M_4 = n\mu_4 + 3n(n-1)\mu_2^2.$$

Hence, Pearson's betas for  $W$ , which are introduced by

$$B_1 = \frac{M_3^2}{M_2^3} \text{ and } B_2 = \frac{M_4}{M_2^2}$$

(cp. with (7)), are related to the corresponding parameters of a single impulse by

$$B_1 = \frac{\beta_1}{n} \text{ and } B_2 = 3 - \frac{3}{n} + \frac{\beta_2}{n}.$$

[42] It is easily seen that the skewness  $B_1$  vanishes and  $B_2$  approaches 3 as the number of impulses increases, in accordance with the central limit theorem.

[43] To analyze this tendency in more detail, it is convenient to use parameters

$$g_1 = M_3/M_2^{3/2} = B_1^{1/2},$$

$$g_2 = M_4/M_2^2 - 3 = B_2 - 3,$$

which are closely related to Pearson betas and are also widely used as estimates of skewness and kurtosis, respectively.

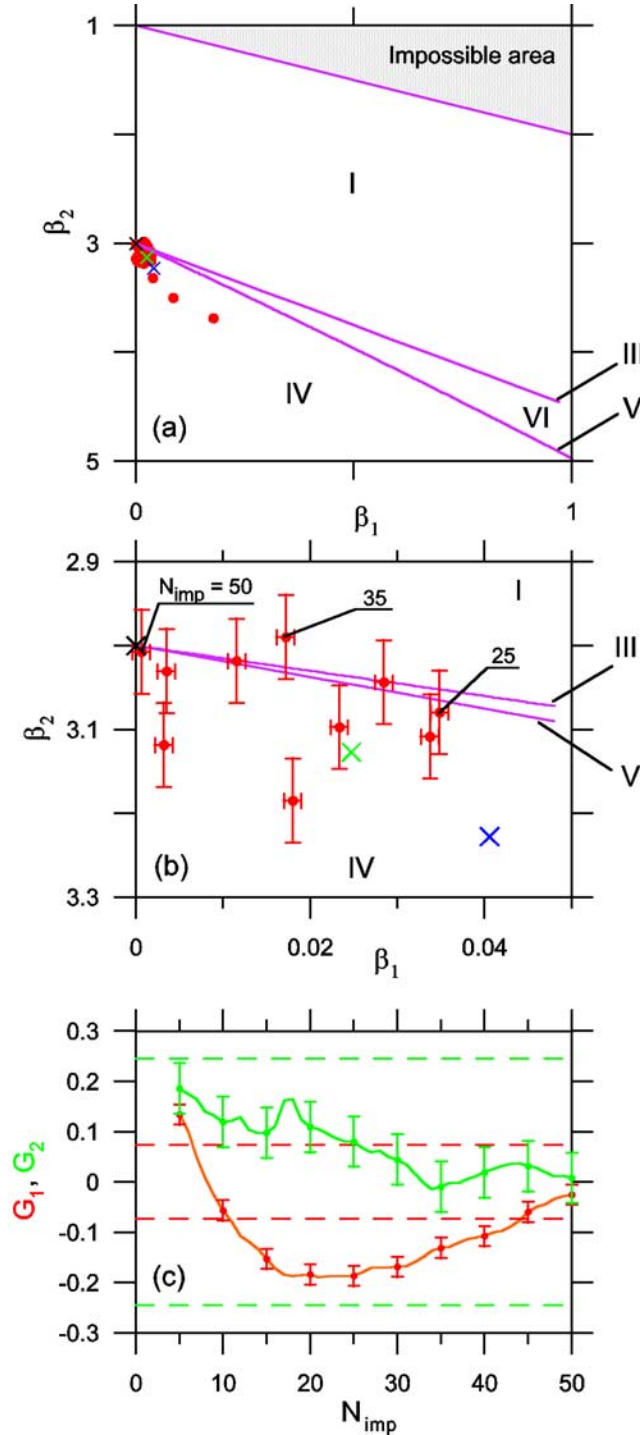


**Figure 3.** (a) The diagram for various types of Pearson distributions, together with the results of numerical simulations (red circles) and experimental data (green and blue crosses correspond to Pearson parameters calculated directly from measurements and from the best fit of the Pearson class IV distribution). The regions corresponding to different distribution classes are denoted by roman numbers. A black cross corresponds to the normal distribution. (b) A small part of previous diagram. For several points shown also are the effective numbers of regions with the positive growth rate,  $N_{imp}$ . A black cross corresponds to normal distribution. (c) Dependence of  $G_1$  (red line) and  $G_2$  (green line) on the effective number of regions (impulses) with the positive growth rate. For normal distributions  $G_1$  and  $G_2$  should vanish; horizontal lines show the corresponding thresholds for deviations to be statistically significant.

[44] For small samples, the unbiased estimates of these parameters are given by (see, e.g., [Lvovski, 1988])

$$G_1 = \frac{\sqrt{n(n-1)}}{n-2} g_1,$$

$$G_2 = \frac{n-1}{(n-2)(n-3)} [(n+1)g_2 + 6],$$

with the corresponding mean square deviations

$$S_{G_1} = \sqrt{\frac{6n(n-1)}{(n-2)(n+1)(n+3)}},$$

$$S_{G_2} = \sqrt{\frac{24n(n-1)^2}{(n-3)(n-2)(n+3)(n+5)}},$$

which are useful when performing a simple test to evaluate an assumption for a distribution to be normal. For normal distributions the following conditions are satisfied [Lvovski, 1988]:

$$|G_1| < 3 S_{G_1}, \quad |G_2| < 5 S_{G_2}. \quad (11)$$

[45] From the data set that was obtained in numerical simulations and was already used in the plot of  $\beta_2$  versus  $\beta_1$  shown in Figure 3, we calculate the dependencies of statistics  $G_1$  and  $G_2$  on the mean number of peaks in the growth rate. These dependencies are shown in the bottom panel of Figure 3, together with the corresponding thresholds in criteria (11). It is easily seen that for the chosen profiles of the growth rate almost everywhere the distribution of  $\log_{10} W$  differs significantly from the normal one, but the difference becomes insignificant for  $N_{\text{imp}}$  as large as 45–50.

[46] With allowance made for statistical scatter of  $\beta_2$  estimates, the data points lie in the region corresponding to type IV distributions (see the middle panel in Figure 3). Additional analysis shows that the corresponding fits based on estimates of moments pass the  $\chi^2$  goodness-of-fit test described in the following section.

[47] It follows from these results that the conditions for applicability of the limiting form of pure stochastic growth theory [Robinson, 1992, 1995; Robinson et al., 1993a, 1993b] could be rather severe, at least in the Earth's foreshock where an estimate for the typical value of the number of growth rate fluctuations is slightly higher than  $\sim 10$  [Cairns and Robinson, 1997].

#### 4. Analysis of Experimental Data and Discussion

[48] In this section, we present an analysis of Langmuir wave amplitudes measured by the WBD instrument aboard the CLUSTER spacecraft on 17 February 2002. The instrument was described by Gurnett et al. [1997]. The available experimental data are band-limited waveforms of electric field, the frequency range is 1–77 kHz and a sampling frequency is equal to 220 kHz. WBD instrument captures waveforms in the form of 10 millisecond snapshots taken every 80 milliseconds.

[49] The electric antenna is positioned in the spin plane of a rotating spacecraft therefore the measured electric field corresponds to a projection of the electric field vector to the direction of the antenna. Assuming that the electrostatic waves are longitudinally polarized and propagate approximately along the ambient magnetic field, the observed amplitudes are corrected by dividing them by a cosine of the angle between the antenna and the magnetic field.

[50] Between 8:20 and 9:22 UT the spacecraft were located not far from the electron foreshock boundary, where unusually intense Langmuir waves ( $|E| > 40$  mV/m) were observed. Deeper in the foreshock, the amplitudes decreased to more typical values, below a few mV/m, and during the time interval from 9:25 to 10:13 UT the measured wave amplitude seems to be approximately stationary, both the mean and variance of the observed amplitudes being relatively constant throughout the whole period considered. Cairns and Robinson [1999] argued that both the average and standard deviation of  $\log W$  have power law dependencies on the distance  $D_f$ , which is measured downstream from the magnetic field tangent line, parallel to the Earth-Sun line, and often called *DIFF*. Boshuizen et al. [2001] showed that aggregating data over a large range of  $D_f$  leads to power law distributions for  $\log W$ . To estimate the variations of  $D_f$ , we use the formulas by Cairns et al. [1997], both for foreshock coordinates and parameters that determine the shock's standoff distance and the perpendicular scale of the shock; the data for magnetic field and solar wind ram pressure at the bow shock nose were provided by CDAWeb facility with the 1-min time resolution (the OMNI data set). Although the distributions obtained for the interval 09:25–10:13 UT of approximate stationarity does not have a power law tail, for further analysis we choose a shorter interval, 9:25–9:47 UT, where  $D_f$  does not change considerably and lies within the range 1.6–4.1  $R_E$ .

[51] During this later interval the WBD instrument was operating on three of the four spacecraft. We only used data from CLUSTER 1 and 3, because on these two spacecraft the instrument was set into an automatic gain control mode, when the gain of the receiver is adjusted in accordance with previously observed amplitudes. On CLUSTER 4 the gain of the receiver was fixed to its lowest value (i.e., all gain amplifiers were removed from the measurement chain), and the data from this mode are not suitable for our analysis due to the limited range of amplitudes that can be measured reliably.

[52] To estimate the probability distribution of wave energies, we built a statistical ensemble from the mean values of  $|E|^2$  in each of the 10 ms snapshots, where  $E$  is the corrected value of the electric field. From this ensemble we removed the snapshots where the data were strongly influenced by instrumental effects (WHISPER sounder interference, receiver saturation, or strong digitization noise). We also omitted all observations where the angle between the antenna and the magnetic field was larger than  $75^\circ$ . For the chosen subinterval of the event under consideration (from 9:25 to 9:47 UT) this procedure yields a statistical ensemble of 10027 values.

[53] To evaluate to what extent the data correspond to proposed probability distributions, we first built a histogram of the energies from the statistical ensemble described above using  $N_b = 30$  logarithmically spaced bins. The

goodness of fit of each distribution is then evaluated using the  $\chi^2$  statistical test [Bendat and Piersol, 2000]. Let  $f(\log W)$  denote the theoretical probability distribution of logarithm of wave energy,  $W_i$  the centers of the bins,  $h_i$  the numbers of observations in each bin, and  $N = \sum h_i$  the total number of observations. The test is based on the observation that if the data follow a given distribution  $f(\log W)$ , then the normalized error of fit

$$X^2 = \sum_{i=1}^{N_b} \frac{[Nf(\log W_i) - h_i]^2}{Nf(\log W_i)} \quad (12)$$

is a random variable with a  $\chi^2$  distribution with the number of degrees of freedom given by  $\nu = N_b - N_p - 1$ , where  $N_p$  is the number of free parameters in the fitted function. We can thus use this quantity to test the hypothesis that the data are distributed according to a predicted distribution function by comparing the value of  $X^2$  to a percentage point of the  $\chi^2$  distribution,  $\chi_{\nu, \alpha}^2$ , at a chosen significance level  $\alpha$ .

[54] In Figure 4, we compare the goodness of fit for a normal distribution and a Pearson type IV distribution in  $\log W$ . The distribution function shown by a red line is a maximum likelihood fit of a normal distribution to the histogram of logarithms of wave energies. The green curve shows the fit of the Pearson type IV distribution whose parameters were calculated using the moment technique outlined by Hahn and Shapiro [1967]. In this approach we first calculated the first four moments of the distribution,  $m_1, \dots, m_4$ , from the time series and substituted the moments into a general formula for a type IV distribution [Tikhonov, 1982; see also Podladchikova et al., 2003]. Formulas (7) then give us the corresponding values of Pearson parameters  $\beta_1 = 0.025$  and  $\beta_2 = 3.13$  whose significance will be discussed later in this section. The blue curve in Figure 4 represents a fit of the Pearson type IV distribution with parameters obtained by maximum likelihood fitting. Here we consider the  $X^2$  error function (12) for a specific case of the type IV distribution and for a histogram built from the experimental data. As the type IV distribution has five degrees of freedom, we find the best fit values of the five unknown parameters by nonlinear minimization of this error function [Press et al., 1992]. The resulting distribution minimizes the error function and therefore provides by definition the best fit with respect to the  $\chi^2$  test. Pearson parameters corresponding to this fitted distribution are  $\beta_1 = 0.041$  and  $\beta_2 = 3.228$ .

[55] From the plots shown in Figure 4 it is clear that the type IV distribution fits the data significantly better than the normal one and the  $X^2$  values corresponding to these 3 fits (66.44, 26.69 and 20.88 respectively) confirm this. To emphasize the differences between the distributions both on the tails and near their peaks, logarithmic and linear scales for probabilities are used. It is easily seen that the type IV distribution are better than normal one throughout the whole wave energy range. The value of the cumulative distribution function  $C = 1 - \text{Prob}[\chi_{\nu}^2 < X^2]$ , quantifying the likelihood that the data under consideration follow the respective theoretical distribution, is relatively small ( $C = 2.15 \cdot 10^{-5}$ ) for the normal distribution and we can thus reject the null hypothesis that the measured  $\log W$  obeys a normal distribution, at a significance level higher than 99.99%. On the other hand, for the two fits of type IV

distribution,  $C$  equals 0.32 for the moment technique fit (green curve) and  $C = 0.65$  for the maximum likelihood fit (blue curve). The statistical hypothesis that the wave energy follows the type IV distribution therefore cannot be rejected even at a significance level of 75%.

[56] One can come to the same conclusion with the use of a simple approach outlined in the previous section. For the data under consideration formulas (7) yield Pearson parameters  $\beta_1 = 0.025$  and  $\beta_2 = 3.13$ . The corresponding data point is shown on the Pearson diagram in Figure 3 by a green cross. The distance to the point corresponding to normal distributions is rather large, thereby assuming that the distribution of wave energy is not lognormal. Indeed, in this case we have also  $G_1 = 0.16$ ,  $G_2 = 0.13$ ,  $S_{G_1} = 0.02$  and  $S_{G_2} = 0.05$ . For the first parameter the ratio of its absolute value to the corresponding standard deviation is higher than 6, while for the second one is equal to 2.7. Thus the first test or normality in (11) fails. Now using the maximum likelihood fit for a type IV distribution, we find  $G_1 = 0.20$ ,  $G_2 = 0.23$ ,  $G_1/S_{G_1} = 8.2$ , and  $G_2/S_{G_2} = 4.7$ . The corresponding data point is shown on the Pearson diagram in Figure 3 by a blue cross. With this fit, the violation of the first criterion in (11) is more significant while the second criterion is not far from being violated. Hence the hypotheses that the distribution under consideration is normal should obviously be rejected. An inequality  $G_1 > 0$  means that the distribution is asymmetrical, with the left tail being less pronounced as compared with the right one, which corresponds to relatively large wave amplitudes.

[57] The distribution for  $\log W$  could be normal under the conditions of applicability of stochastic growth theory, where it was assumed that the number of fluctuations in growth rate during a characteristic wave residence time is large enough for the central limit theorem to hold. However, from the results outlined in the previous section it follows that the conditions for applicability of this theory could be rather severe. Thus we can argue that the observed distribution is not normal because the central limit theorem fails for the event considered. If this is the case, then the empirical distribution should depend on a lot of different factors like the effective number of inhomogeneities, their shape etc. These distributions cannot be fit by a normal one because the latter is too simple and depends only on 2 parameters, the mean and variance. To obtain an adequate fit, one should take into consideration more complicated distributions. The classification based on Pearson curves depending on 4 parameters seems to be appropriate for analysis of such data.

[58] Unfortunately, the WBD measurements are performed rather sparsely and this hampers finding events suitable for more studies. Nevertheless, another Cluster experiment, WHISPER, provides the measurements of electric field spectra with much larger coverage. The problem of testing the predictions of SGT theory as well as of appropriateness of Pearson classification of Langmuir wave spectra in the Earth's foreshock with the Whisper data will be addressed in future studies.

## 5. Conclusions

[59] A numerical model of wave propagation in unstable plasma with inhomogeneities was developed. This model

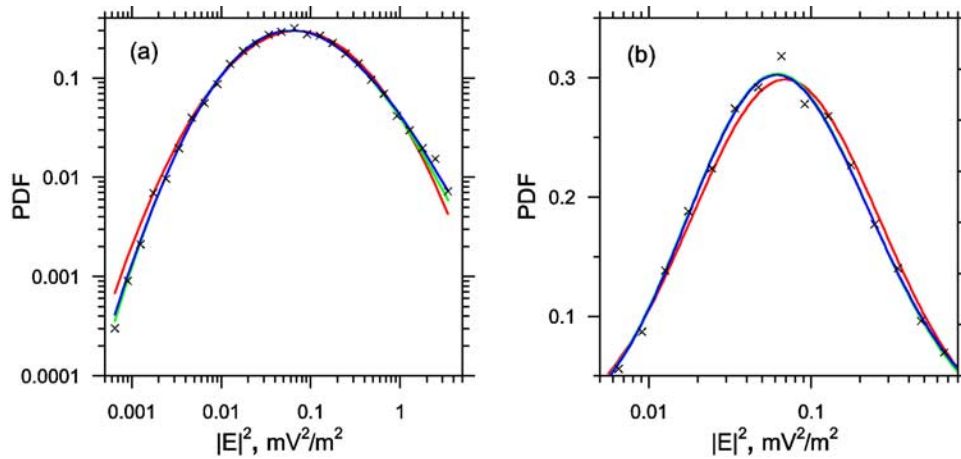


**Figure 4.** Probability density function (PDF) for the logarithm of Langmuir wave energy density for the period 9:25–9:47 UT on February 17, 2002, when CLUSTER spacecraft was within the Earth’s electron foreshock (black crosses). The red line shows the maximum likelihood fit of a normal distribution. The green and blue lines correspond to fits of Pearson type IV distribution. The fit shown by the blue line was obtained by the maximum likelihood method, while for another fit shown by the green line the parameters were calculated from the estimates of moments for empirical distribution. Logarithmic (a) and linear (b) scales for PDFs are used, to show the differences between the distributions both on the tails and near their peaks.

describes the linear interaction of Langmuir wave packets with an electron beam in randomly inhomogeneous plasma. Two effects were taken into account, i.e., angular diffusion of the wave vector on small-amplitude density fluctuations and suppression of instability caused by the removal of the wave from the resonance with particles during crossing of density perturbations of relatively large amplitude.

[60] Using this model, we studied the spatial evolution of the wave packet shape in plasmas with a beam and the results obtained were used to model a shot-noise-like stochastic process composed of such packets. To analyze both numerical and experimental data, a Pearson technique was used to determine the type of spectral density distributions. It was shown that both experimental and model distributions for the logarithm of wave energy belong to a Pearson type IV rather than to a normal one as was previously stated by *Robinson* [1995] [see also *Cairns and Robinson*, 1997 and references therein]. *Robinson’s* conclusion was derived from the central limit theorem applied to logarithms of wave energy. We suggest that the main reason for formation of more complicated distributions than the normal one is that the effective number of regions where the waves grow is not very large and, as a consequence, the central limit theorem fails to be true under the typical conditions for the Earth’s electron foreshock. In this case the statistical properties of the wave energy distributions depend on a lot of different details, in particular, on the shapes of the growth rate profiles, the effective number of regions with positive growth rate etc. To analyze the deviations of the observed distributions for  $\log W$  from the normal one, it is convenient to use Pearson’s classification of distributions. It is worth pointing out that the characteristics of the distributions such as the higher order moments together with the angular width can be used to evaluate the relative role of the angular diffusion due to small-amplitude density fluctuations and characteristic

number of growth/damping regions along the wave path if these two effects are dominant. The corresponding technique is suitable for distributions with one extremum. It is based on estimates of the first four moments of empirical distributions and seems to have an optimal flexibility for describing space experimental data. On the contrary, the normal distribution depends only on two parameters, mean and variance, and it is appropriate under the restrictive condition that the central limit theorem applies.

[61] For large amplitudes, it is suggested that power law tails can result from variations of wave amplitudes due to changes of group velocity in the inhomogeneous plasma, in particular due to reflection of waves from inhomogeneities.

[62] **Acknowledgments.** This work was partially supported by le Studium program of Region Centre of France. The work of K. Musatenko was supported by French Government Fellowship. J. Soucek acknowledges the support of grants IAA301120601 and IAA300420602 of Grant Agency of the Academy of Science of the Czech Republic. J. Pickett acknowledges support from NASA GSFC under Grant NNG04GB098G. Iver Cairns acknowledges financial support from the Australian Research Council.

[63] Amitava Bhattacharjee thanks the reviewers for their assistance in evaluating this paper.

## References

- Bale, S. D., D. Burgess, P. J. Kellogg, K. Goetz, and S. J. Monson (1997), On the amplitude of intense Langmuir waves in the terrestrial electron foreshock, *J. Geophys. Res.*, *102*, 11,281–11,286.
- Bale, S. D., P. J. Kellogg, K. Goetz, and S. J. Monson (1998), Transverse Z-mode waves in the terrestrial electron foreshock, *Geophys. Res. Lett.*, *25*, 9.
- Bale, S. D., D. E. Larson, R. P. Lin, P. J. Kellogg, K. Goetz, and S. J. Monson (2000), On the beam speed and wavenumber of intense electron plasma waves near foreshock edge, *J. Geophys. Res.*, *105*, 27,353–27,367.
- Bendat, J. S., and A. G. Piersol (2000), *Random data, analysis and measurement procedures*, Wiley, New York.
- Boshuizen, C. R., I. H. Cairns, and P. A. Robinson (2001), Stochastic growth theory of spatially-averaged distributions of Langmuir fields in Earth’s foreshock, *Geophys. Res. Lett.*, *28*(18), 3569–3572.
- Cairns, I. H. (2004), Properties and interpretation of giant micropulses and giant pulses from pulsars, *Astrophys. J.*, *610*, 948–955.

- Cairns, I. H., and P. A. Robinson (1997), First test of stochastic growth theory for Langmuir waves in Earth's foreshock, *Geophys. Res. Lett.*, *24*(4), 369–372.
- Cairns, I. H., and P. A. Robinson (1999), Strong evidence for stochastic growth of Langmuir-like waves in the Earth's foreshock, *Phys. Rev. Lett.*, *82*, 3066–3069.
- Cairns, I. H., P. A. Robinson, R. R. Anderson, and R. J. Strangeway (1997), Foreshock Langmuir waves for unusually constant solar wind conditions: Data and implications for foreshock structure, *J. Geophys. Res.*, *102*, 24,249–24,264.
- Cairns, I. H., P. A. Robinson, and R. R. Anderson (2000), Thermal and driven stochastic growth of Langmuir-like waves in the solar wind and Earth's foreshock, *Geophys. Res. Lett.*, *27*, 61–64.
- Celnikier, L. M., C. C. Harvey, R. Jegou, M. Kemp, and P. Moricet (1983), A determination of the electron fluctuation spectrum in the solar wind, using the ISEE propagation experiment, *Astron. Astrophys.*, *126*, 293–298.
- Celnikier, L. M., L. Muschietti, and M. V. Goldman (1987), Aspects of interplanetary plasma turbulence, *Astron. Astrophys.*, *181*, 138–154.
- Cronyn, W. M. (1970), The analysis of radio scattering and space-probe observations of small-scale structure in the interplanetary medium, *Astrophys. J.*, *161*, 755–763.
- Gilbert, E. N., and H. O. Pollak (1960), Amplitude distribution of shot noise, *The Bell system technical*, 333–350.
- Gurnett, D. A., R. R. Anderson, F. L. Scarf, and W. S. Kurth (1978), The heliocentric radial variation of plasma oscillations associated with type III radio bursts, *J. Geophys. Res.*, *83*, 4147–4152.
- Gurnett, D. A., R. F. Hulf, and D. L. Kirchner (1997), The wide-band plasma wave investigation, *Space Sci. Rev.*, *79*, 95–208.
- Hahn, G. H., and S. S. Shapiro (1967), *Statistical Models in Engineering*, Wiley, New York.
- Kellogg, P. J., and T. S. Horbury (2005), Rapid density fluctuations in the solar wind, *Annales Geophysicae*, *23*, 3765–3773.
- Kellogg, P. J., K. Goetz, S. J. Monson, and S. D. Bale (1999), Langmuir waves in a fluctuating solar wind, *J. Geophys. Res.*, *104*, 17,069–17,078.
- Khazanov, G. V., T. Neubert, and G. D. Gefan (1994), A unified theory of ionosphere-plasmasphere transport of suprathermal electrons, *IEEE Trans. Plasma Sci.*, *22*, 187–198.
- Li, B., P. A. Robinson, and I. H. Cairns (2006a), Numerical simulations of type-III solar radio bursts, *Phys. Rev. Lett.*, *96*, 145,005.
- Li, B., P. A. Robinson, and I. H. Cairns (2006b), Numerical modeling of type-III solar radio bursts in the inhomogeneous solar corona and interplanetary medium, *Phys. Plasmas*, *13*, 092,902.
- Lin, R. P., D. W. Potter, D. A. Gurnett, et al. (1981), Energetic electrons and plasma waves associated with a solar type III radio burst, *Astrophys. J.*, *251*, 364–373.
- Lvovski, E. N. (1988), *Statistical methods for obtaining empirical formulas*, Vysshaya Shkola, Moscow (in Russian).
- Melrose, D. B., G. A. Dulk, and I. H. Cairns (1986), Clumpy Langmuir waves in type III solar radio bursts, *Astron. Astrophys.*, *163*, 229–238.
- Mishin, E. V., A. A. Trukhan, and G. V. Khazanov (1990), *Plasma effects of superthermal electrons in the ionosphere*, Nauka, Moscow (in Russian).
- Muschietti, L., M. V. Goldman, and D. Newman (1985), Quenching of the beam-plasma instability by large-scale density fluctuations in 3 dimensions, *Solar Physics*, *96*, 181–198.
- Nishikawa, K., and D. D. Ryutov (1976), Relaxation of relativistic electron beam in a plasma with random density inhomogeneities, *J. Phys. Soc. Japan*, *41*, 1757–1765.
- Pearson, K. (1895), Contributions to the Mathematical Theory of Evolution. II. Skew Variation in Homogeneous Material., *Philos. Trans. R. Soc. A*, *186*, 343–414.
- Podladchikova, O., B. Lefebvre, V. Krasnoselskikh, and V. Podladchikov (2003), Classification of probability densities on the basis of Pearson's curves with application to coronal heating simulations, *Non. Proc. Geophys.*, *10*(4/5), 323–333.
- Press, W. H., S. A. Teukolsky, W. T. Vetterling, and B. P. Flannery (1992), *Numerical Recipes in C: The Art of Scientific Computing*, Cambridge Univ. Press, New York.
- Rice, S. O. (1944), Mathematical analysis of random noise, *The Bell Systems Technical J.*, *23*, 282–332.
- Robinson, P. A. (1992), Clumpy Langmuir waves in type III radio sources, *Solar Physics*, *139*, 147–163.
- Robinson, P. A. (1995), Stochastic wave growth, *Phys. Plasmas*, *2*, 1466–1479.
- Robinson, P. A., I. H. Cairns, and D. A. Gurnett (1993a), Clumpy Langmuir waves in type III radio sources: comparison of stochastic-growth rate theory with observations, *Astrophys. J.*, *407*, 790–800.
- Robinson, P. A., A. J. Willis, and I. H. Cairns (1993b), Dynamics of Langmuir and ion-sound waves in type III solar radio sources, *Astrophys. J.*, *408*, 720–734.
- Robinson, P. A., B. Li, and I. H. Cairns (2004), New regimes of stochastic wave growth, *Phys. Rev. Lett.*, *93*, 235003, doi:10.1103/PhysRevLett.93.235003.
- Salpeter, E. E. (1967), Interplanetary scintillations. I. Theory, *Astrophys. J.*, *147*, 433–448.
- Sigsbee, K., C. A. Kletzing, D. A. Gurnett, J. S. Pickett, A. Balogh, and E. Lucek (2004), The dependence of Langmuir wave amplitudes on position in Earth's foreshock, *Geophys. Res. Lett.*, *31*, L07805, doi:10.1029/2004GL019413.
- Smith, D. F. (1977), Second harmonic radiation and related nonlinear phenomena in type III solar radio bursts, *Astrophys. J.*, *216*, L53–L57.
- Smith, D. F., and D. Sime (1979), Origin of plasma-wave clumping in type III solar radio burst sources, *Astrophys. J.*, *233*, 998–1004.
- Soucek, J., V. Krasnoselskikh, T. Dudok de Wit, J. Pickett, and C. Kletzing (2005), Nonlinear decay of foreshock Langmuir waves in the presence of plasma inhomogeneities: Theory and Cluster observations, *J. Geophys. Res.*, *110*, A08102, doi:10.1029/2004JA010977.
- Tikhonov, V. I. (1982), *Statistical Radioengineering*, Moscow, Radio i Sviaz (in Russian).

I. H. Cairns, University of Sydney, Sydney, Australia.

V. V. Krasnoselskikh, V. V. Lobzin, and K. Musatenko, LPCE/CNRS-Université d'Orléans, 3A Avenue de la Recherche Scientifique, 45071, Orléans, CEDEX 2, France. (vkrasnos@cns-orleans.fr)

J. S. Pickett, University of Iowa, IA, USA.

J. Soucek, Institute of Atmospheric Physics, Prague, Czech Republic.